Angular phase plate analyzers for measuring the dimensionality of multi-mode fields

Pors, J.B.; Aiello, A.; Oemrawsingh, S.S.R.; Exter, M.P. van; Eliel, E.R.; Woerdman, J.P.

Angular phase-plate analyzers for measuring the dimensionality of multimode fields

J. B. Pors,* A. Aiello, S. S. R. Oemrawsingh, M. P. van Exter, E. R. Eliel, and J. P. Woerdman
Huygens Laboratory, P.O. Box 9504, 2300 RA Leiden, The Netherlands
(Received 7 November 2007; published 26 March 2008)

Analyzers comprised of an angular phase plate and a single-mode fiber have recently been introduced to study the angular profile of optical fields. Here, we quantify the number of degrees of freedom, or modes, that such an analyzer can resolve. Its performance is described by means of an angular coherence function and we introduce a dimensionality that gives the effective number of modes that a given analyzer can probe. This quantity can, as we show experimentally, easily be retrieved from a dual analyzer setup.

DOI: 10.1103/PhysRevA.77.033845 PACS number(s): 42.79.−e, 42.40.Eq, 42.50.Dv

I. INTRODUCTION

Over the last fifteen years, impressive advance has been made on wavefront control of optical fields. A striking example of this progress is found in the technique of adaptive optics imaging [1], where a spatial light modulator [2] or micromirror array [3] performs dynamic wavefront corrections on an impinging field. Currently, several devices, known as diffractive optical elements, are available to manipulate or analyze the azimuthal phase profile of a beam. Among these are angular phase plates [4–6] and amplitude holograms [7–9] or phase holograms [10,11]. An angular phase plate is a transmissive (or reflective) plate whose optical thickness has a purely angular variation, hence imprinting into a field an azimuthally dependent phase retardation. When the angular variation of the optical thickness is superimposed with a spatial carrier frequency, we deal with a phase hologram.

In recent years, the azimuthal phase dependence of optical fields has drawn much attention, both from a fundamental and applied perspective. It was realized that the azimuthal phase profile of a paraxial electromagnetic field can be identified with the orbital angular momentum carried by that field ($m\hbar$ per photon, with m a discrete index) [12,13]. Nowadays, orbital-angular-momentum states find their application in optical tweezers [14,15], in cold-atom physics [16], and in the manipulation of Bose-Einstein condensates [17,18], where they are utilized to rotate samples.

Orbital-angular-momentum states, of which there are infinitely many, were also addressed in twin-photon experiments [19,20], motivated by the advantages that quantum entanglement in a high-dimensional mode space might provide for quantum-information science [21]. The experiments employed similar field analyzers composed of a diffractive optical element, a focusing lens and a single-mode fiber that is coupled to a photodetector. The important aspect introduced in Ref. [20] was to rotate the diffractive element around the propagation axis of the field. In the current paper, we will investigate this class of field analyzers, in particular, regarding their capability to measure the dimensionality of an incident field by rotating the diffractive element.

As mentioned above, the angular phase operation performed on the field can be realized with either an amplitude or phase hologram [19] or an angular phase plate [20]. Although these devices are in many respects very similar, the use of a phase hologram in a field analyzer as described above has a drawback because of the beam deflection that is inherent to its operation; when the hologram is to be rotated, it would imply that the fiber must be translated, which greatly complicates a practical implementation. In contrast, phase plates are purely zero-order devices and hence do not suffer from this disadvantage. We will therefore, without loss of generality, assume that the diffractive phase object be a phase plate.

Thus, the field analyzer we are concerned with comprises, successively, a rotatable angular phase plate, a focusing lens, a single-mode fiber, and a photodetector. A crucial property of the analyzer is that it performs a single-mode detection for any orientation of the phase plate. This selection goes under the name of "spatial filtering" or "projective measurement" in classical and quantum optics, respectively, and is enforced by the single-mode fiber, which exclusively sustains a Gaussian mode carrying no orbital angular momentum ($m=0$). Note that the analyzer can be applied to both classical and quantum fields, if intensity measurements are performed with a photodiode or single-photon detector, respectively. For the current argument, we will simply speak of a photodetector.

The detection state of the analyzer as a whole is given by the fiber's Gaussian mode combined with the angular phase plate's operation. This detection state can be expanded in the orbital-angular-momentum eigenmodes of the field so as to reveal its modal content, with expansion coefficients carrying both amplitude and phase. The amplitudes of these complex coefficients are fixed by the physical profile of the phase object; they are "engraved" in the plate. The phase components, in contrast, depend on the orientation angle of the device. The analyzer's detection state can be readily customized by designing the appropriate phase plate. For instance, pure orbital-angular-momentum states (integer m) can be selected using so-called spiral phase plates of integer order [4]. This kind of plate acts as a pure ladder operator in orbital-angular-momentum space and increases (or decreases) the orbital angular momentum of the field by an integer multiple of $\hbar$ per photon. Field analyzers equipped with these plates constitute a special class; their expansion in field eigenmodes contains merely one term, and their operation is therefore invariant under rotation of the plate. It was in fact this kind of transformation that was exploited in Ref. [19] (be it by

*pors@molphys.leidenuniv.nl

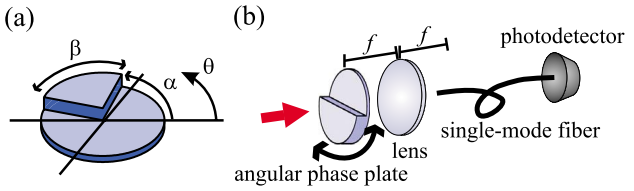

FIG. 1. (Color online) (a) Heaviside step phase plate with arc sector β producing a phase shift π with respect to the remainder of the plate. The plate orientation is denoted by α and θ is the azimuthal coordinate. (b) Angular phase-plate analyzer with Heaviside step phase plate having $\beta=\pi$. The impinging field diffracts from the angular phase plate and is coupled to a single-mode fiber by a lens of focal length f. The phase plate can be rotated.

using a fork-shaped phase hologram, rather than a spiral phase plate). The detection state of a general analyzer, however, is typically a superposition of numerous, if not infinitely many orbital-angular-momentum eigenmodes (as, for example, for the noninteger spiral phase plate used in Ref. [20]). In that case, the phases of the various modes will evolve each in their individual way when the plate's orientation angle is varied. As a consequence, the detection state alters as the phase plate is rotated and the analyzer thus scans a potentially high-dimensional mode space.

In this article, we aim to gain a deeper understanding of this behavior. In particular, we address the question how to quantify the number of spatial modes, or dimensionality, that such a field analyzer can resolve. In order to do so, we first represent the single-mode analyzer by a mutual coherence function and derive an expansion in orbital-angular-momentum eigenmodes. We then discuss the commonly used fidelity dimension D_{fid}, which counts the *total* number of modes that can be observed by this type of field analyzers [22]. Subsequently, we introduce a measure D_{eff} that gives the *effective* number of angular degrees of freedom that can be resolved. It can be interpreted as the number of information channels available, be it in a nontrivial way. The effective dimensionality is, unlike the fidelity dimension, independent of experimental conditions. We show that this number can straightforwardly be retrieved from a dual analyzer setup and we present experimental data that confirm this.

II. HEAVISIDE STEP PHASE PLATE

To illustrate our general theory, we will apply our findings at several moments in this article to a Heaviside step phase plate analyzer [23,24]. We therefore first introduce this specific angular phase-plate analyzer.

A Heaviside step phase plate is a transmissive (or reflective) plate having an arc sector whose optical thickness is half a wavelength greater than the remainder of the plate [see Fig. 1(a)]. The part of the field that crosses this arc sector thus flips sign. The length of the arc section producing the π phase shift is given by the parameter β. The plate's transmission function can simply be written as

$$t(\theta,\alpha) = 1 - 2[\Theta(\theta-\alpha) - \Theta(\theta-\alpha-\beta)]. \tag{1}$$

Here $\Theta(x)$ is the Heaviside step function, θ is the azimuthal coordinate, and α is the orientation angle of the phase plate. The angles θ and α are both measured from the positive direction of a reference axis and are periodic in 2π. A special case is given by $\beta=\pi$, in which case the plate consists of two equal halves of phase difference π. The corresponding phase operation connected to such a plate is the well-known Hilbert transformation [25].

Assembling an angular phase plate, a coupling lens, a single-mode fiber and a photodetector leads to our field analyzer. The phase plate and single-mode fiber are placed in their mutual far field, at a focal distance f on either side of the incoupling lens. An illustration of an analyzer equipped with a Heaviside plate of arc sector $\beta=\pi$ is shown in Fig. 1(b).

III. DETECTION-STATE EXPANSION IN ORBITAL-ANGULAR-MOMENTUM EIGENMODES

We consider a monochromatic paraxial field of wavelength $\lambda=2\pi/k$, propagating along the z axis of an optical system. It can be written in the form

$$\psi(r,\theta,z,t) = V(r,\theta)\exp[i(kz-\omega t)], \tag{2}$$

where $V(r,\theta)$ is the complex amplitude of the field and (r,θ,z) are cylindrical coordinates defined with respect to the z axis of the system. We aim to analyze the azimuthal dependence of $V(r,\theta)$ with an field analyzer of the kind described above.

The phase plate performs a purely angular phase operation on the field that is unitary and is represented by a transmission function $t(\theta,\alpha)=\exp[i\phi(\theta,\alpha)]$, where $\phi(\theta,\alpha)$ describes the azimuthal phase dependence and α is the orientation angle of the plate. We note that radial degrees of freedom may in principle be incorporated by allowing for an overall radial dependence that is decoupled from the angular part, yet this is beyond the scope of the current paper. The fiber is placed in the Fourier plane of the phase plate, where the orbital-angular-momentum field components are radially separated. It exclusively supports a single mode, which we approximate by a Gaussian profile $V_0(r)/\sqrt{2\pi}$, where $V_0(r)=(2/w_0)\exp[-r^2/w_0^2]$, and w_0 is the beam waist. The fiber filters this mode, which depends on the radial coordinate only and thus corresponds to the $m=0$ orbital-angular-momentum component, from an impinging field.

We are free to consider the product of the fiber mode and the phase plate's transformation as our detection state. We define the *detection dual field*:

$$U(r,\theta,\alpha) = V_0(r)\frac{1}{\sqrt{2\pi}}t(\theta,\alpha), \tag{3}$$

which is the detection state of the composite measurement device. The dual field has a straightforward physical meaning: It is the field emerging from the phase plate when the single-mode fiber is fed in the backward direction (i.e., from the photodetector side) with the fundamental Gaussian. This important property will be exploited later to build an experimental setup for measuring D_{eff}.

The strength of the coupling, quantified by $P(\alpha)$, between the analyzer and an impinging field is given by the mode-overlap integral

$$P(\alpha) = \left| \int V^*(r,\theta) U(r,\theta,\alpha) r dr d\theta \right|^2. \quad (4)$$

The power measured by the detector can thus be calculated as the overlap integral between the input field $V(r,\theta)$ and the detection dual field $U(r,\theta,\alpha)$. Formulated alternatively, the input field is projected onto the detection state.

Due to the fact that the analyzer selects one particular radial mode, that does not depend on the orientation α of the plate, it is justified to restrict our attention to the angular content of the detection state. We therefore define the normalized *angular* detection dual field as $A(\theta,\alpha) = t(\theta,\alpha)/\sqrt{2\pi}$.

An important property of this field is its rotational symmetry

$$\hat{R}(\alpha) A(\theta,0) = A(\theta,\alpha) = A(\theta-\alpha,0), \quad (5)$$

where $\hat{R}(\alpha) = \exp(i\alpha \hat{L}_z)$ is the rotation operator representing a counterclockwise rotation about z by an angle α; $\hat{L}_z = \frac{1}{i}\frac{\partial}{\partial\theta}$ is the orbital-angular-momentum operator [26]. Now, let us assume that for a given input field we perform intensity measurements $P(\alpha)$ for several angular settings α of the phase plate. To each plate setting $\alpha = \alpha_i$ corresponds a dual field $A(\theta,\alpha_i)$, and to a whole set of orientations $\{\alpha_1,\alpha_2,\ldots\}$ corresponds a set of detection dual fields $\{A(\theta,\alpha_1), A(\theta,\alpha_2),\ldots\}$. That is to say that, as α is varied, an ensemble of different realizations of the field $A(\theta,\alpha)$ is constructed. It is customary in optics to describe ensembles by means of their mutual coherence function [27]. Along similar lines, we introduce an angular coherence function [28] $\gamma(\theta_1,\theta_2) = \langle A(\theta_1,\alpha) A^*(\theta_2,\alpha)\rangle_\alpha$, where the brackets $\langle\cdots\rangle_\alpha$ denote averaging with respect to the angle α. Since α is a continuous parameter, we can write this as

$$\gamma(\theta_1,\theta_2) = \frac{1}{2\pi}\int_0^{2\pi} A(\theta_1,\alpha) A^*(\theta_2,\alpha) d\alpha, \quad (6)$$

normalized to $\int_0^{2\pi}\gamma(\theta,\theta)d\theta = 1$. This is the first main result of this paper: It furnishes an explicit and simple recipe to represent a given analyzer by a partially coherent field described by a angular coherence function $\gamma(\theta_1,\theta_2)$.

Next, we apply the methods of image-analysis theory [29] to determine the participating degrees of freedom of such a field. These methods are based on the fact that the mutual coherence function is a Hilbert-Schmidt kernel, Hermitian, and positive semidefinite, which follows from its definition and its rotational symmetry [Eq. (6)] [27]. Then, a modal decomposition is always possible and $\gamma(\theta_1,\theta_2)$ may be expressed as

$$\gamma(\theta_1,\theta_2) = \sum_m \gamma_m u_m(\theta_1) u_m^*(\theta_2). \quad (7)$$

The functions $u_m(\theta)$ are the eigenfunctions and the coefficients $\gamma_m \geq 0$ are the eigenvalues of the homogeneous Fredholm integral equation $\int_0^{2\pi}\gamma(\theta,\theta')u_m(\theta')d\theta' = \gamma_m u_m(\theta)$. The modal decomposition is particularly simple thanks to the cylindrical symmetry of the functions $A(\theta,\alpha)$. In fact, the field modes are just the orbital angular momentum eigenfunctions of $\hat{L}_z$:

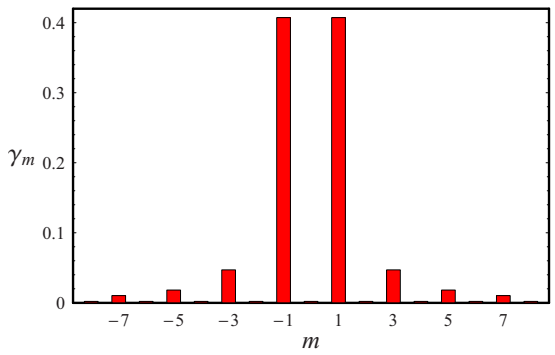

FIG. 2. (Color online) Modal decomposition of the detection dual field for an analyzer equipped with a Heaviside step phase plate, with $\beta = \pi$. The histogram shows the distribution of the eigenvalues γ_m for the orbital angular momentum states $u_m(\theta)$.

$$u_m(\theta) = \frac{1}{\sqrt{2\pi}}\exp(im\theta), \quad (8)$$

with $m = 0, \pm 1, \pm 2, \ldots, \pm\infty$. The eigenvalues γ_m are given by the modulus square of the Fourier coefficients of $A(\theta,0)$:

$$\gamma_m = \frac{1}{2\pi}\left| \int_0^{2\pi} A(\theta,0) e^{-im\theta} d\theta \right|^2. \quad (9)$$

The eigenvalues γ_m give the coupling strength, or sensitivity of the analyzer to the field mode $u_m(\theta)$. The set complies the natural normalization condition

$$\sum_m \gamma_m = 1. \quad (10)$$

For the example of an analyzer equipped with a Heaviside step phase plate, we find

$$\gamma_m = \begin{cases} (1-\beta/\pi)^2, & m = 0, \\ \dfrac{4}{m^2\pi^2}\sin^2(m\beta/2), & m \neq 0. \end{cases} \quad (11)$$

In Fig. 2 we show the spectrum of eigenvalues for $\beta = \pi$. This distribution contains ample information about the expected performance of the field analyzer. For example, if the input field has no angular dependence, it will not couple at all with this analyzer, since $\gamma_0 = 0$. Second, as the Heaviside plate has an antisymmetric profile on the domain $0 < \theta < 2\pi$, all even m terms vanish.

IV. DIMENSIONALITY

In an actual experimental setting every field mode $u_m(\theta)$ is subject to a certain amount of noise. A mode $u_m(\theta)$ can thus only be detected if the analyzer's coupling efficiency to that mode γ_m is sufficiently large [30]. Hence, there is a *total* number of detectable modes, that is, the number of modes whose detection efficiency exceeds their noise level, which is referred to as the fidelity dimension D_{fid} [22]. One should

bear in mind that this measure only has a useful meaning if the field is expanded in the eigenmodes of the system. The fidelity dimension has some merit, as it gives the number of modes needed to describe an analyzer's dual field to a noise-limited accuracy [24]. Notwithstanding, it is clear that this dimension is not an absolute measure of the analyzer's performance, as the noise level depends on the exact experimental conditions. For example, the noise could be suppressed by prolonging the measurement time, hence increasing D_{fid}.

Instead, we now introduce an alternative definition that does have an absolute meaning. It relies on the fact that, generally, modes do not participate equally. Returning to Fig. 2, it is clear that there are two dominant modes ($m=\pm 1$) and two subdominant ones ($m=\pm 3$) [and two sub-subdominant ones ($m=\pm 5$), etc.]. Thus, we expect that the *average* number of detectable modes will be larger than 2, but not much larger. To quantify this number, let us note that if $\gamma(\theta_1,\theta_2)$ had exactly D nonzero eigenvalues uniformly distributed, $\gamma_1=\gamma_2=\ldots=\gamma_D$, the normalization condition would impose $\gamma_m=1/D \quad (m=1,\ldots,D)$. As a consequence, the Hilbert-Schmidt norm of such a finite-dimensional distribution would just be $\Sigma_{m=1}^{D}\gamma_m^2=1/D$. Inspired by this result, we define the average number of detectable modes or *effective dimensionality* D_{eff} of the field analyzer, as

$$D_{\mathrm{eff}}=\frac{1}{\sum_{m=-\infty}^{\infty}\gamma_m^2}. \tag{12}$$

This dimensionality can be interpreted as the number of channels available for communication purposes [31,32], although they are not individually accessible. It is worth noting that this definition is actually independent of experimental conditions.

When we apply this formula to the distribution given in Eq. (11), we obtain after a straightforward calculation

$$D_{\mathrm{eff}}(\beta)=\begin{cases}1/[1-4\beta/\pi+6(\beta/\pi)^2-(8/3)(\beta/\pi)^3], & \beta\in[0,\pi],\\ D_{\mathrm{eff}}(2\pi-\beta), & \beta\in[\pi,2\pi].\end{cases} \tag{13}$$

The effective dimensionality ranges between 1 and 6. In the specific case of the distribution reported in Fig. 2, we find $D_{\mathrm{eff}}(\beta=\pi)=3$, consistent with our intuitive reasoning.

As a second example, we return to the analyzer equipped with a spiral phase plate of integer order n. It selects a pure orbital angular momentum state: $\gamma_m=\delta_{nm}$, with δ_{ij} the Kronecker delta. The resultant effective dimensionality equals $D_{\mathrm{eff}}=1$, exposing the inability of this apparatus to probe a multidimensional space. Equation (12) is the second main result of this paper. It furnishes a simple recipe to calculate the number of modes that an angular phase plate analyzer can effectively detect.

V. MEASURING THE EFFECTIVE DIMENSIONALITY

The effective dimensionality D_{eff}, defined in Eq. (12), can actually be measured with the simple experimental setup shown in Fig. 3. The setup consists of a mirror-inverted field analyzer, oriented at α', that is imaged by means of a telescope onto a normal field analyzer oriented at α. With mirror-inverted field analyzer, we mean that the analyzer is equipped with an angular phase plate that is a mirrored copy of the normal angular phase plate. More details on the setup can be found in Ref. [24]. With this scheme, we can basically measure the overlap between two analyzer modes belonging to different phase plate orientations α and α'. From the definition of the detection dual field given previously, it follows that the mirror-inverted analyzer generates a dual field $A(\theta,\alpha')$, when fed from the output port of its fiber. This field is imaged onto the second analyzer that selects the dual field $A(\theta,\alpha)$ and relays an output signal whose power equals

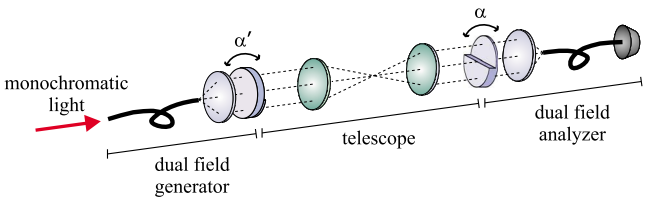

FIG. 3. (Color online) Setup for the determination of the effective dimensionality D_{eff}. Monochromatic light emerges from a mirror-inverted field analyzer oriented at an angle α', and is coupled into a normal field analyzer set at α. The intensity is recorded as α is rotated over 2π. Here, the phase plates have a Heaviside step profile, with $\beta=\pi$.

$$P(\alpha,\alpha')=\left|\int_0^{2\pi}A^*(\theta,\alpha)A(\theta,\alpha')\mathrm{d}\theta\right|^2\equiv|G(\alpha,\alpha')|^2. \tag{14}$$

The rotational symmetry [Eq. (5)] yields a direct correspondence between $G(\alpha-\alpha')$ and the analyzer's coherence function: $G(\alpha,\alpha')=2\pi\gamma(-\alpha,-\alpha')$. In fact, it follows that

$$G(\alpha,\alpha')=G(\alpha-\alpha'). \tag{15}$$

The coupling strength between the mode generator and mode analyzer is, not surprisingly, dependent on the relative orientation angle $\alpha-\alpha'$ only. The coherence function $G(\alpha,\alpha')$ is a measure of the angular sensitivity of a mode analyzer, meaning that it characterizes how fast the detection mode changes when the phase plate is rotated.

Figure 4 shows intensity measurements obtained with a dual detector setup for our Heaviside step phase plate analyzer (with $\beta=\pi$) [24]. The dots are experimental data and the solid curve gives the theoretical mode overlap $|G(\alpha-\alpha')|^2$. The coherence $G(\alpha-\alpha')$ changes linearly with the difference angle $\alpha-\alpha'$, giving rise to a parabolic intensity curve.

Exploiting the correspondence with $\gamma(\alpha,\alpha')$ and its expansion in orbital-angular-momentum eigenmodes, we integrate $G(\alpha-\alpha')$ over the difference angle $\alpha-\alpha'$ and arrive at

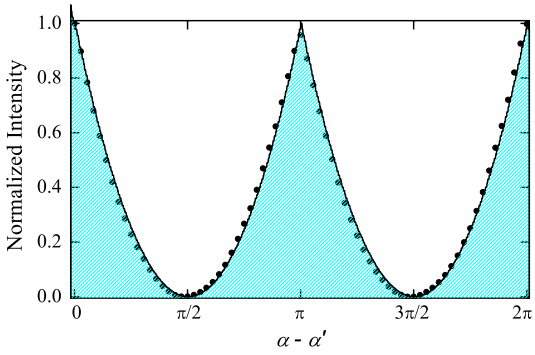

FIG. 4. (Color online) Experimental determination of the effective dimensionality D_{eff} of a Heaviside step phase plate analyzer with $\beta=\pi$, by means of the setup depicted in Fig. 3. The dots are experimental data (taken from Ref. [24].) and the solid curve the theoretically predicted $|G(\alpha-\alpha')|^2$. The value of D_{eff} is the inverse of the average normalized intensity (equal to 2π divided by the area underneath the normalized curve).

$$D_{\text{eff}} = \frac{2\pi}{\int_0^{2\pi} |G(\alpha-\alpha')|^2 \mathrm{d}(\alpha-\alpha')}. \tag{16}$$

That is to say, the effective dimensionality D_{eff} of the detector is just equal to 2π times the inverse of the area below the curve of normalized maximum intensity. This shows the experimental relevance of the newly defined effective dimensionality. Applying this strategy to the case shown in Fig. 4, we find indeed $D_{\text{eff}}=3.0$, in agreement with theory. Equation (16) is the third major result of this paper.

VI. DISCUSSION

We have demonstrated that the angular phase plate analyzers under consideration show multiple aspects regarding dimensionality: They are (i) single-mode projectors, (ii) able to access high-dimensional spaces, and (iii) characterized by an effective dimensionality D_{eff}. Here, we aim to give an intuitive representation of these features.

The key idea in this section is to represent a detection dual field $A(\theta,\alpha)$ by a complex vector in the linear, infinite-dimensional space $\cup$ that is spanned by the orbital angular momentum modes $u_m(\theta)$. The detection state vector has components along the "axes" $u_m(\theta)$ that carry both amplitude and phase.

The coupling sensitivity of the field analyzer to a mode $u_m(\theta)$, given by an amplitude γ_m, is set by the physical shape of the phase plate. Thus, as all γ_m are fixed, the modal content of the dual field is fixed. This reflects the single-mode detection of the analyzer.

However, the performance of these analyzers is not determined by a single value of $A(\theta,\alpha)$ calculated for a given value of the continuous parameter α, but rather by the whole set of fields $\{A(\theta,\alpha)\}_\alpha$ obtained by varying α between 0 and 2π. When the phase plate is rotated, the state vector $A(\theta,\alpha)$ redirects, as the phase factors of each field component $u_m(\theta)$ start to change. As a result, the set of fields $\{A(\theta,\alpha)\}_\alpha$ spans a subspace $\cup_\alpha \subseteq \cup$ that occupies some "volume" within $\cup$. Our effective dimensionality D_{eff} quantifies this volume, by weighing the eigenmodes $u_m(\theta)$ in the expansion of $A(\theta,\alpha)$ by the square of their coefficients γ_m.

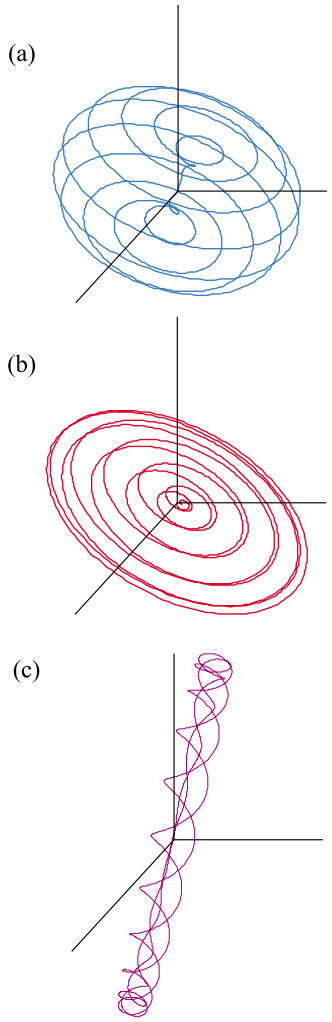

FIG. 5. (Color online) Graphical representation of the effective dimensionality. Although all three curves, representing different sets of detection dual fields, make excursions along all three axes, only (a) spans a three-dimensional object. The curves in (b) and (c) span objects of dimensionality close to 2 and 1, respectively.

In Fig. 5 we sketch the behavior of $A(\theta,\alpha)$ in a cartoon-like manner. For pictorial convenience, we fix this figure to $\dim(\cup)=3$ and we draw $A(\theta,\alpha)$ as a real-valued three-dimensional vector. As the parameter α varies, such a vector draws a continuous curve within $\cup$, and after a 2π rotation of α it returns at its initial point. The closed curve makes excursions in all three dimensions and so it spans an overall object. When this curve embodies a ball-like volume, as in Fig. 5(a), it implies that all γ_m are approximately equal and the effective dimensionality of this volume is about 3. However, the excursions may not be equally strong along all axes. When the spanned structure spans a platelike volume, squeezed along a certain direction, as shown in Fig. 5(b), its effective dimensionality is about 2. Finally, when the curve

covered by $A(\theta,\alpha)$ spans a cigarlike space squeezed along two directions, as depicted in Fig. 5(c), then $D_{\text{eff}} \simeq 1$.

VII. CONCLUSION

The key results of this paper are threefold. First, we have shown that an angular phase-plate analyzer can be represented by an angular coherence function [Eq. (6)] and we have given its expansion in orbital-angular-momentum eigenmodes. Second, we have introduced a novel quantity that gives the effective number of modes that an analyzer can access [Eq. (12)]. Unlike the fidelity dimension, which counts the total number of observable modes in the presence of noise, the effective dimensionality does not depend on experimental conditions. It can be seen as the number of communication channels that an analyzer sustains. Lastly, it was shown that the effective dimensionality can easily be obtained experimentally. This important feature is expressed by Eq. (16).

Moreover, we have suggested an intuitive picture of how to represent the analyzer's detection state as a vector in an infinite-dimensional mode space. The insight in the properties of angular phase plate analyzers paves the way to design analyzers that scan high-dimensional mode spaces, applicable to the analysis of both classical and quantum fields.

ACKNOWLEDGMENTS

We thank Johan de Jong for earlier measurements used for Fig. 4. This project was supported by the Stichting voor Fundamenteel Onderzoek der Materie.

[1] R. K. Tyson, *Principles of Adaptive Optics* (Academic Press, San Diego, 1998).
[2] U. Efron, *Spatial Light Modulator Technology (Optical Engineering)* (Marcel Dekker, New York, 1995).
[3] D. J. Dagel, W. D. Cowan, O. B. Spahn, G. D. Grossetete, A. J. Grine, M. J. Shaw, P. J. Resnick, and B. Jokiel Jr, J. Microelectromech. Syst. **15**, 572 (2006).
[4] M. W. Beijersbergen, R. P. C. Coerwinkel, M. Kristensen, and J. P. Woerdman, Opt. Commun. **112**, 321 (1994).
[5] S. S. R. Oemrawsingh, J. A. W. van Houwelingen, E. R. Eliel, J. P. Woerdman, E. J. K. Verstegen, J. G. Kloosterboer, and G. W. 't Hooft, Appl. Opt. **43**, 688 (2004).
[6] C. Rotschild, S. Zommer, S. Moed, O. Hershcovitz, and S. G. Lipson, Appl. Opt. **43**, 2397 (2004).
[7] V. Y. Bazhenov, M. V. Vasnetsov, and M. S. Soskin, JETP Lett. **54**, 492 (1990).
[8] N. R. Heckenberg, R. McDuff, C. P. Smith, and A. G. White, Opt. Lett. **17**, 221 (1992).
[9] *Optical Vortices*, edited by M. Vasnetsov and K. Staliunas (Nova Science Publishers, Commack, NY, 1999).
[10] H. He, N. R. Heckenberg, and H. Rubinsztein-Dunlop, J. Mod. Opt. **42**, 217 (1995).
[11] J. Arlt, K. Dholakia, L. Allen, and M. J. Padgett, J. Mod. Opt. **45**, 1231 (1998).
[12] L. Allen, M. W. Beijersbergen, R. J. C. Spreeuw, and J. P. Woerdman, Phys. Rev. A **45**, 8185 (1992).
[13] J. Leach, M. J. Padgett, S. M. Barnett, S. Franke-Arnold, and J. Courtial, Phys. Rev. Lett. **88**, 257901 (2002).
[14] H. He, M. E. J. Friese, N. R. Heckenberg, and H. Rubinsztein-Dunlop, Phys. Rev. Lett. **75**, 826 (1995).
[15] N. B. Simpson, K. Dholakia, L. Allen, and M. J. Padgett, Opt. Lett. **22**, 52 (1997).
[16] S. Kuppens, M. Rauner, M. Schiffer, K. Sengstock, W. Ertmer, F. E. van Dorsselaer, and G. Nienhuis, Phys. Rev. A **58**, 3068 (1998).
[17] K. T. Kapale and J. P. Dowling, Phys. Rev. Lett. **95**, 173601 (2005).
[18] M. F. Andersen, C. Ryu, P. Cladé, V. Natarajan, A. Vaziri, K. Helmerson, and W. D. Phillips, Phys. Rev. Lett. **97**, 170406 (2006).
[19] A. Mair, G. W. A. Vaziri, and A. Zeilinger, Nature (London) **412**, 313 (2001).
[20] S. S. R. Oemrawsingh, X. Ma, D. Voigt, A. Aiello, E. R. Eliel, G. W. 't Hooft, and J. P. Woerdman, Phys. Rev. Lett. **95**, 240501 (2005).
[21] D. Kaszlikowski, P. Gnaciński, M. Żukowski, W. Miklaszewski, and A. Zeilinger, Phys. Rev. Lett. **85**, 4418 (2000).
[22] R. Jozsa, J. Mod. Opt. **41**, 2315 (1994).
[23] R. Danev, H. Okawara, N. Usuda, K. Kametani, and K. Nagayama, J. Biol. Phys. **28**, 627 (2002).
[24] S. S. R. Oemrawsingh, J. A. de Jong, X. Ma, A. Aiello, E. R. Eliel, G. W. 't Hooft, and J. P. Woerdman, Phys. Rev. A **73**, 032339 (2006).
[25] S. Lowenthal and Y. Belvaux, Appl. Phys. Lett. **11**, 49 (1967).
[26] J. J. Sakurai, *Modern Quantum Mechanics* (Addison-Wesley, Reading, MA, 1994).
[27] L. Mandel and E. Wolf, *Optical Coherence and Quantum Optics*, 1st ed. (Cambridge University Press, Cambridge, 1995).
[28] C. Paterson, Phys. Rev. Lett. **94**, 153901 (2005).
[29] G. T. di Francia, J. Opt. Soc. Am. **59**, 799 (1969).
[30] C. W. Helstrom, J. Opt. Soc. Am. **60**, 521 (1970).
[31] F. Gori and G. Guattari, Opt. Commun. **7**, 163 (1973).
[32] D. A. B. Miller, Appl. Opt. **39**, 1681 (2000).